

A New ^{18}F -Labeled Folic Acid Derivative with Improved Properties for the PET Imaging of Folate Receptor–Positive Tumors

Tobias L. Ross¹, Michael Honer¹, Cristina Müller², Viola Groehn³, Roger Schibli¹, and Simon M. Ametamey¹

¹Animal Imaging Center–PET, Center for Radiopharmaceutical Science of ETH, PSI, and USZ, Institute of Pharmaceutical Science, ETH Zürich, Zürich, Switzerland; ²Center for Radiopharmaceutical Science of ETH, PSI, and USZ, Paul Scherrer Institute, Villigen PSI, Switzerland; and ³Merck & Cie, Schaffhausen, Switzerland

The folate receptor is a proven target for folate-based diagnosis and treatment of cancer. Several folic acid conjugates have been developed as radiopharmaceuticals, but a suitable ^{18}F -labeled folic acid derivative for routine clinical use is still lacking. The purpose of this study was to investigate the potential of 2'- ^{18}F -fluorofolic acid as a PET agent for folate receptor–positive tumors. **Methods:** The binding affinity of the cold reference compound 2'-fluorofolic acid was determined by in vitro displacement assays using human folate receptor–positive KB cells and ^3H -folic acid. ^{18}F labeling of 2'-fluorofolic acid was accomplished via a direct nucleophilic aromatic substitution of *N*-(*N*,*N*-dimethylamino-methylene)-2'-nitrofolate di-*tert*-butylester followed by acidic cleavage of the amino and carboxylic protecting groups. The new radiofolate was evaluated in nude mice bearing KB tumor xenografts under control and blocking conditions. Animals were either scanned from 75 to 105 min after injection of the radiotracer or sacrificed 75 min after injection for ex vivo biodistribution studies. **Results:** 2'-fluorofolic acid showed a high binding affinity (inhibition constant, 1.8 ± 0.1 nM) for the folate receptor. Direct aromatic ^{18}F labeling of 2'-fluorofolic acid was achieved within 80 min via a convenient 2-step procedure in satisfactory radiochemical yields. The new radiotracer exhibited excellent pharmacokinetics with fast renal clearance and only moderate hepatobiliary elimination. Uptake of 2'- ^{18}F -fluorofolic acid in folate receptor–positive KB tumors was high and specific, allowing a clear-cut visualization by PET. **Conclusion:** 2'- ^{18}F -fluorofolic acid, obtained via an integrated approach, is a promising PET agent for folate receptor–positive tumors and outperforms previously reported ^{18}F -labeled folates.

Key Words: folic acid; folate receptor; ^{18}F ; PET; pemetrexed

J Nucl Med 2010; 51:1756–1762

DOI: 10.2967/jnumed.110.079756

Folic acid, vitamin B₉, is required in eukaryotic cells in its reduced forms as a cofactor for de novo DNA synthesis in which they act as a 1-carbon source (1). In general, cells use 3 different mechanisms for folate uptake. Under physiologic conditions, healthy cells transport folates mainly via membrane-spanning proteins, the reduced folate carrier and the proton-coupled folate transporter, directly into the cytosol. The proton-coupled folate transporter is highly expressed in the duodenum and jejunum, where it transports folates preferentially at low pH values (2). The reduced folate carrier displays only a low, micromolar affinity for the oxidized forms of folic acid, whereas the reduced forms of folic acid have a high affinity for the reduced folate carrier (3). In pathophysiologic situations, highly proliferating cells such as cancer cells additionally express a 38-kDa glycoprotein receptor, the folate receptor, which internalizes folic acid by endocytosis. The folate receptor exhibits high affinity (dissociation constant [K_d], ~ 1 nM) for folic acid in its oxidized form and lower affinity for reduced folates (3,4). The membrane-anchored folate receptor isoform α of this receptor (α -folate receptor) is associated with various epithelial malignancies such as ovarian and endometrial carcinomas, breast cancer, and lung cancer and can reach immensely elevated expression levels, whereas its physiologic expression in healthy tissues is highly restricted to only the choroid plexus, lungs, kidneys, and placenta (4–6).

Over the past 2 decades, the utility of folic acid for targeting the α -folate receptor on epithelial cancer cells has been demonstrated using folate-conjugated chemotherapeutics and imaging agents (7–9). Several folate-conjugated radiopharmaceuticals have been synthesized and evaluated successfully using imaging modalities such as SPECT and PET (9). All these folate radiopharmaceuticals have been labeled via conjugation to folic acid, and most of them are metal complexes of radionuclides such as $^{99\text{m}}\text{Tc}$ (10–12), ^{111}In (13), and $^{66/67/68}\text{Ga}$ (14,15).

In general, folate-based radiopharmaceuticals show a high radiotracer accumulation in the kidneys due to a physiologic folate receptor expression in proximal tubule cells (16). Recently, Müller et al. reported a favorable effect of the

Received Jun. 1, 2010; revision accepted Aug. 5, 2010.

For correspondence or reprints contact: Simon M. Ametamey; Animal Imaging Center–PET, Center for Radiopharmaceutical Science of ETH, PSI, and USZ, Institute of Pharmaceutical Sciences, ETH Zürich; Wolfgang-Pauli-Strasse 10, 8093 Zürich, Switzerland.

E-mail: simon.ametamey@pharma.ethz.ch.

COPYRIGHT © 2010 by the Society of Nuclear Medicine, Inc.

antifolate pemetrexed on kidney and tumor uptake (17,18); thus, the high radioactivity accumulation and the potential risk of damage to the kidneys may no longer be an issue.

The first ^{18}F -labeled folate derivative, α/γ - ^{18}F -4-fluorobenzylamine (FBA) folate (Supplemental Fig. 1) (supplemental materials are available online only at <http://jnm.snmjournals.org>), was developed by our group and synthesized via a non- α/γ -regioselective conjugation of 4- ^{18}F -fluorobenzylamine to folic acid (19). However, the multistep radiosynthesis and the accompanying low radiochemical yield limited the potential for routine use. More recently, we reported another ^{18}F -labeled folate conjugate designated ^{18}F -click folate (Supplemental Fig. 1) (20). An efficient 2-step procedure provided the ^{18}F -click folate in high radiochemical yields of 25%–35% in less than 90 min. Although ^{18}F -click folate showed good tumor uptake and high specificity for folate receptor, it was accompanied by a strong hepatobiliary excretion that resulted in high abdominal background radioactivity.

So far, all ^{18}F -labeled folic acid derivatives described have been prepared via a conjugate approach by coupling prosthetic groups to the carboxylate functionality in the glutamate moiety of folic acid. Our aim was to adapt a direct ^{18}F -labeling strategy (integrated approach) whereby the newly developed ^{18}F -labeled derivative would closely resemble folic acid and lack a prosthetic group. An option was the direct introduction of the ^{18}F label at the 2'-position of the 4-amino-benzoyl moiety in folic acid. Here, we describe the radiosynthesis and the preclinical evaluation of 2'- ^{18}F -fluorofolic acid (Supplemental Fig. 1) as a high-affinity and specific PET ligand for imaging folate receptor–positive tumors. Additionally, we report the effect of the antifolate pemetrexed on kidney and tumor uptake of 2'- ^{18}F -fluorofolic acid.

MATERIALS AND METHODS

Reagents and solvents were purchased from Sigma-Aldrich Chemie GmbH or VWR International AG. All chemicals were used as supplied unless stated otherwise. The precursor, N^2 -(N,N -dimethylaminomethylene)-2'-nitrofolate di-*tert*-butylester (Fig. 1), and the reference compound, 2'-fluorofolic acid (21), were generously provided by Merck & Cie. ^3H -folic acid was purchased from Moravex Biochemicals Inc. Human KB cells were obtained from DSMZ.

Analytic radio-high-performance liquid chromatography (HPLC) was performed on an Agilent 1100 series HPLC system

equipped with a GabiStar (Raytest) radiodetector using an RP-18 column, Gemini 5- μm C18 (Phenomenex), 250×4.6 mm, with a solvent system and gradient as follows: Eluent A was an aqueous 0.05 M NaH_2PO_4 solution that was adjusted to pH 7.0 by the addition of 1 M sodium hydroxide solution, and eluent B was methanol. The gradient was from 85% eluent A to 5% eluent A at 0–12 min, 5% eluent A at 12–15 min, and from 5% eluent A to 85% eluent A at 15–24 min. Specific radioactivity was determined from a calibration curve obtained from different concentrations of the cold reference compound 2'-fluorofolic acid (Supplemental Fig. 2).

Semipreparative radio-HPLC was performed on an HPLC system equipped with a Merck-Hitachi L-6200A intelligent pump, a Knauer variable-wavelength ultraviolet detector and an Eberline RM-14 radiodetector. 2'- ^{18}F -fluorofolic acid was purified on a reversed-phase column, Gemini 5- μm C18 (Phenomenex), 250×10 mm, using a gradient as follows: eluent A was an aqueous 0.05 M NaH_2PO_4 solution that was adjusted to pH 7.0 by the addition of 1 M sodium hydroxide solution, and eluent B was methanol. The gradient was from 98% eluent A to 40% eluent A at 0–30 min and from 40% eluent A to 10% eluent A at 30–40 min.

Radio-thin-layer chromatography (TLC) was performed on silica-coated polyester sheets (Polygram SIL G/UV₂₅₄; Macherey-Nagel). A solution of triethylamine (1%) in methanol was used as mobile phase. TLCs were analyzed on an Instant Imager system (Canberra).

PET was performed with the 16-module variant of the quad-HIDAC tomograph (Oxford Positron Systems). This small-animal PET camera provides an ultrahigh resolution of less than 0.9 mm^3 (22).

Production of No-Carrier-Added ^{18}F -Fluoride

No-carrier-added ^{18}F -fluoride was produced via the $^{18}\text{O}(\text{p},\text{n})^{18}\text{F}$ nuclear reaction at a Cyclone 18/9 cyclotron (IBA). Isotopically 97% enriched ^{18}O -water was irradiated by an 18-MeV proton beam using a 2.1-mL target. The target volume was transferred to a hot cell using a helium stream. No-carrier-added ^{18}F -fluoride (~ 80 – 100 GBq) was trapped on an anion exchange cartridge (Sep-Pak Light Accell Plus QMA; Waters AG), preconditioned with 5 mL of aqueous 0.5 M potassium carbonate solution and 5 mL of water.

Synthesis of No-Carrier-Added 2'- ^{18}F -Fluorofolic acid

The no-carrier-added ^{18}F -fluoride trapped on the anion exchange cartridge was directly eluted into a 10-mL sealed reaction vessel using a solution of potassium carbonate (1 mg) and Kryptofix 2.2.2 (5 mg) in 1.5 mL of acetonitrile and water (4:1). The solvents were removed at 85°C – 90°C under a vacuum and a stream of nitrogen. Subsequently, 0.8–1.0 mL of dry acetonitrile was added 3 times and evaporated to dryness.

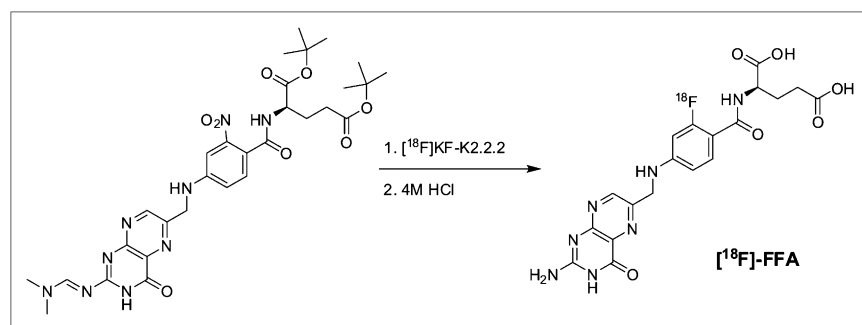


FIGURE 1. Radiosynthesis of 2'- ^{18}F -fluorofolic acid ($[^{18}\text{F}]\text{-FFA}$).

To the dry ^{18}F -fluoride-cryptate complex the precursor, N^2 -(N , N -dimethylaminomethylene)-2'-nitrofollic acid di-*tert*-butylester (5.2 mg, 8 μmol), in 0.25 mL of dimethylformamide was added. The mixture was heated to 140°C–145°C for 20 min. After 5 min of cooling and the addition of 8 mL of water, the mixture was passed through a reversed-phase cartridge (Sep-Pak C18 Plus; Waters AG). The cartridge was washed 3 times with 10 mL of water and dried for 2 min using a stream of nitrogen. The ^{18}F -labeled protected intermediate, N^2 -(N , N -dimethylaminomethylene)-2'- ^{18}F -fluorofolic acid di-*tert*-butylester, was eluted with 2.5 mL of acetonitrile into another 10-mL sealed reaction vessel. The volume of acetonitrile was concentrated to 0.3 mL under reduced pressure and a nitrogen stream at 80°C–90°C.

For hydrolysis, 0.5 mL of 4 M hydrogen chloride solution was added and the mixture was heated to 60°C for 12 min. After cooling, the mixture was neutralized with 0.5 mL of 4 M sodium hydroxide solution. Half a milliliter of 0.15 M phosphate buffer solution was added, and the mixture was filled with HPLC eluent A to a total volume of 5 mL and was injected into the semipreparative radio-HPLC column. The product fraction was collected, and the mobile phase was evaporated under reduced pressure and a stream of nitrogen at 80°C–90°C. For formulation, water and 0.15 M phosphate buffer solution were added to the dry product and the mixture was passed through a sterile filter into a sterile, pyrogen-free vial.

In Vitro Binding Affinity Assays

Binding affinity assays were performed with KB cells derived from human nasopharyngeal epidermal carcinoma known to overexpress the folate receptor (4). The cells were cultured as monolayers in 75-cm² flasks at 37°C in a humidified atmosphere with 5% CO₂. The cells were kept under folate-starved conditions in a special folate-deficient RPMI 1640 medium (FFRPMI 1640; Cell Culture Technologies) supplemented with heat-inactivated fetal calf serum (10%), L-glutamine, penicillin (100 IU/mL), and streptomycin (100 $\mu\text{g}/\text{mL}$). The fetal calf serum was the only source of folate in the medium to provide a final folate concentration of about 3 pM, which is at the low end of the physiologic serum concentration in humans (23).

Binding assays were performed after a growing phase of 2–3 d when a constant cell growth was reached. A cell suspension in pure FFRPMI 1640 medium (no additives, ice-cold) was distributed to 1.5-mL vials (~7,000 cells and ~240 μL per vial). The cells were incubated in triplicates with ^3H -folic acid (0.84 nM) and increasing concentrations of the nonradioactive reference compound 2'-fluorofolic acid (5.0×10^{-7} to 5.0×10^{-12} M) at 2°C–4°C for 30 min. Nonspecific binding was determined in the presence of native folic acid (10^{-3} M). After incubation, the suspension was centrifuged at 800g and 4°C for 10 min and the supernatant was removed. By addition of 0.5 mL of 1 M NaOH, the cell pellets were resuspended and lysed at the same time. The lysed cells were stirred in a vortex mixer and transferred into scintillation tubes containing 4 mL of scintillation cocktail (Ultima Gold; Perkin Elmer). Radioactivity was measured using a β -counter (LS6500; Beckman), and the inhibitory concentrations of 50% were determined from displacement curves using Origin 8.0 software (OriginLab Corp.). Inhibition constants (K_i values) were calculated according to the Cheng–Prusoff equation (24) using a K_d of ^3H -folic acid of 1 nM.

In Vivo Experiments

Animals. Animal studies complied with Swiss and local laws on animal protection and husbandry. NMRI nude mice (Charles

River) were kept under a folate-deficient rodent diet to reduce their serum concentration of folate to a level comparable to human serum levels (23). After an acclimatization period, the mice were inoculated with 0.1 mL of a KB tumor cell suspension in phosphate-buffered saline (PBS) (5×10^6 cells/mL) into the right axilla of each animal. After a 10- to 14-d growing period, the KB tumors had reached a weight of 80–300 mg and the animals were used for the experiments.

Ex Vivo Biodistribution Studies. 2'- ^{18}F -fluorofolic acid (~1 MBq, ~42 pmol) in PBS was injected into each animal via a lateral tail vein. In the blockade group ($n = 4$), each animal received an excess of folic acid (200 μg in 100 μL of PBS) via intravenous injection 10 min before the radiotracer. The control group ($n = 4$) received an injection of PBS only. Animals were sacrificed by decapitation 75 min after radiotracer injection. Tumors, organs, and tissues were dissected, and the accumulated radioactivity was measured in a γ -counter (Wizard; PerkinElmer). The incorporated radioactivity was expressed as percentage injected dose (%ID) per gram of tissue.

Ex Vivo Metabolite Studies. 2'- ^{18}F -fluorofolic acid (30–60 MBq, 1.3–2.5 nmol) in PBS was injected into each animal ($n = 4$) via a lateral tail vein. Animals were sacrificed by decapitation 15 and 90 min after radiotracer injection. Blood and urine were taken, and tumors were dissected. Whole blood was separated into plasma and cells by centrifugation. Proteins in plasma and in urine were denatured by the addition of methanol and separated by centrifugation. The supernatants were analyzed by radio-HPLC and radio-TLC. Tumor tissue was homogenized in a small volume of PBS using a PT 1200 C Polytron (Kinematica AG) for about 1 min at speed 4. After centrifugation, the supernatant was separated and proteins were denatured by the addition of methanol and removed by centrifugation. The supernatant was analyzed by radio-HPLC and radio-TLC.

Effect of Pemetrexed on Ex Vivo Biodistribution. 2'- ^{18}F -fluorofolic acid (~1 MBq, ~42 pmol) in PBS was injected into each animal via a lateral tail vein. In the antifolate group, each animal ($n = 3$) received 400 μg of pemetrexed via intravenous injection 1 h before radiotracer administration. The control group ($n = 3$) received an injection of only 2'- ^{18}F -fluorofolic acid. At 75 min after injection, the animals were sacrificed by decapitation. Tumors, organs, and tissues were dissected, and the accumulated radioactivity was measured in a Wizard γ -counter and expressed as %ID/g.

In Vivo PET. PET was performed with the 16-module variant of the quad-HIDAC tomograph (22). The animals were injected with 5–8 MBq (210–336 pmol) of 2'- ^{18}F -fluorofolic acid via a lateral tail vein. In the blockade group ($n = 3$), excess folic acid (200 μg in 100 μL of PBS) was injected intravenously 10 min before the radiotracer, and the control group ($n = 3$) received the corresponding volume of PBS only. The animals were anesthetized with isoflurane (Abbott) in an air–oxygen mixture and scanned as described previously (25). The PET scans were acquired from 75 to 105 min after injection for optimal tumor visualization.

RESULTS

Radiochemistry

2'-fluorofolic acid was labeled with ^{18}F via a direct nucleophilic aromatic substitution of the 2'-nitro group of N^2 -(N , N -dimethylaminomethylene)-2'-nitrofollic acid di-*tert*-butylester with ^{18}F -KF-Kryptofix 2.2.2, followed by

acidic cleavage of the amino and carboxylic protecting groups (Fig. 1). The initial step involving the nucleophilic aromatic ^{18}F -fluorination was performed in dimethylformamide at 140°C – 145°C for 20 min to afford the protected ^{18}F -labeled intermediate in a maximum decay-corrected yield of 8%.

The second and final step involving the acidic hydrolysis of the intermediate (4 M HCl at 60°C for 12 min) gave the target compound in 50% maximal decay-corrected yield. The product was purified by semipreparative radio-HPLC and formulated in physiologic buffer solution. Maximal overall decay-corrected yield was about 4%. Quality control by analytic radio-HPLC showed that the radiochemical purity was always greater than 95% and the specific activity averaged 23.7 ± 12.2 GBq/ μmol . The total synthesis time was 80 min, and the identity of 2'- ^{18}F -fluorofolic acid was confirmed by coinjection with the reference compound 2'-fluorofolic acid.

Relative Lipophilicity

For the assessment of the relative lipophilicity, the retention factor (k' value) of **1** (Fig. 1) was determined on a reversed-phase HPLC system. The same HPLC system was already used in previous studies for the determination of the relative lipophilicity of native folic acid ($k' = 0.30$), α/γ -FBA folate (both regioisomers: $k' = 0.67$), and F-click folate ($k' = 2.28$) (20). For 2'-fluorofolic acid, a k' value of 0.53 was obtained. This value is the second lowest after native folic acid and points to a relatively low lipophilicity.

In Vitro Binding Affinity Assays

The mean inhibitory concentration of 50% obtained for 2'-fluorofolic acid from 3 independent experiments was 3.4 ± 0.3 nM ($K_i = 1.8 \pm 0.1$ nM). In the same assay, folic acid exhibited an inhibitory concentration of 50% of 1.1 ± 0.4 nM

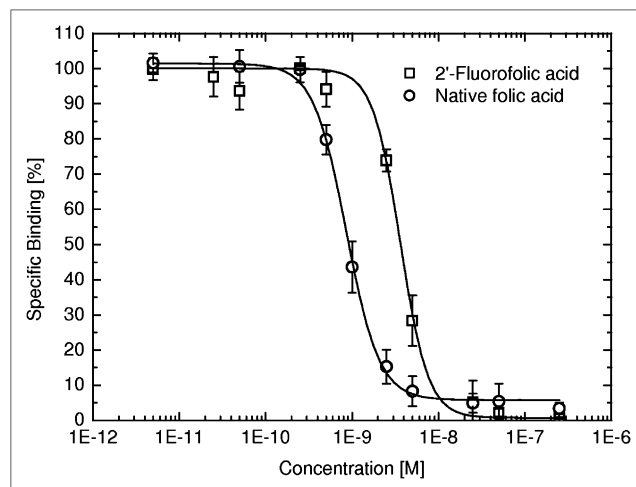


FIGURE 2. Displacement curves of folic acid and 2'-fluorofolic acid using human KB cells (mean \pm SD of percentage specific binding). ^3H -folic acid (0.84 nM) was used as radioligand, and non-specific binding was determined with excess folic acid (10^{-3} M).

($K_i = 0.6 \pm 0.2$ nM) (20). The displacement curves of 2'-fluorofolic acid and folic acid are depicted in Figure 2.

Ex Vivo Biodistribution Studies

Nude mice bearing KB tumor xenografts on their right shoulder were injected with 2'- ^{18}F -fluorofolic acid and sacrificed 75 min after injection. In the control group, KB tumor xenografts showed a radiotracer uptake of 9.37 ± 1.76 %ID/g, which was reduced to 1.20 ± 0.65 %ID/g (87% specificity) under blockade conditions (Table 1). Specific accumulation of the radiotracer was also found in the kidneys. In control animals, radioactivity accumulation in the kidney was 46.06 ± 13.39 %ID/g. This value was clearly reduced to 8.68 ± 11.44 %ID/g in the blockade group. The highest absolute radioactivity concentrations

TABLE 1
Ex Vivo Biodistribution Studies in Nude Mice Bearing KB Tumor Xenografts

Organ or tissue	Control group (n = 4)	Blockade group (n = 4)	Ratio of control to blockade
Lung	1.32 ± 0.20	0.66 ± 0.63	2.00 ± 2.21
Liver	7.79 ± 1.23	5.87 ± 2.23	1.33 ± 0.71
Kidney	46.06 ± 13.39	8.68 ± 11.44	5.31 ± 8.54
Brain	0.50 ± 0.12	0.05 ± 0.03	10.00 ± 8.40
Heart	1.32 ± 0.20	0.32 ± 0.27	4.13 ± 4.11
Spleen	1.60 ± 0.46	0.40 ± 0.28	4.00 ± 3.95
Stomach	1.73 ± 0.22	0.45 ± 0.39	3.84 ± 3.82
Intestine	2.80 ± 0.76	2.23 ± 0.88	1.26 ± 0.84
Bone	1.59 ± 0.11	0.97 ± 0.43	1.64 ± 0.84
Blood	0.40 ± 0.08	0.166 ± 0.63	0.61 ± 0.70
Urine	50.29 ± 29.10	169.64 ± 111.71	0.30 ± 0.37
Feces	5.82 ± 3.01	7.08 ± 2.04	0.82 ± 0.66
Gallbladder	17.69 ± 10.35	24.66 ± 11.73	0.72 ± 0.76
KB tumor	9.37 ± 1.76	1.20 ± 0.65	7.81 ± 5.70

In blockade group, each animal received 200 μg of folic acid 10 min before radiotracer injection. All animals were sacrificed 75 min after injection, and data are expressed as %ID/g.

were found in the kidneys and urine. Radioactivity uptake in the bile and intestine/feces was relatively low, suggesting that renal elimination is the predominant excretion pathway. Moreover, a remarkable blocking effect was also found in the brain, heart, and spleen.

Ex Vivo Metabolite Studies

Nude mice bearing KB tumor xenografts on their right shoulder were injected with 2'-¹⁸F-fluorofolic acid and sacrificed at 15 and 90 min after injection. Plasma, urine, and tumor tissue were analyzed for radiometabolites using radio-HPLC and radio-TLC. A set of typical HPLC chromatograms are depicted in Supplemental Figure 3. Unaltered parent compound, 2'-¹⁸F-fluorofolic acid, and 1 major radiometabolite with increased hydrophilicity were found in all samples (Table 2). The analysis indicated that less than 20% of the radioactivity in urine at 15 and 90 min after injection was parent compound. Plasma samples at both time points showed that 60%–70% of the radioactivity derived from a radiometabolite that was more hydrophilic than the parent compound. In tumor tissue extracts, 34% and 18% of the radioactivity was associated with the parent compound at 15 and 90 min after injection, respectively. The extraction method used was suitable because radioactivity recovery was efficient.

Effect of Pemetrexed on Ex Vivo Biodistribution

Antifolate injection 1 h before radiotracer injection had only a marginal effect on KB tumor uptake. Radioactivity in the tumor decreased only slightly, from 11.50 ± 0.28 %ID/g to 8.65 ± 3.05 %ID/g (Table 3), whereas the unfavorably high kidney uptake was reduced by 61%, that is, from 35.73 ± 0.25 %ID/g to 14.05 ± 1.02 %ID/g. Radioactivity uptake in the liver and feces was also remarkably reduced, by 57% and 50%, respectively, whereas gallbladder uptake remained almost unchanged after pemetrexed preinjection.

In Vivo PET

PET studies performed on nude mice bearing KB tumor xenografts showed high uptake of 2'-¹⁸F-fluorofolic acid in the α -folate receptor–positive tumors and folate receptor–

TABLE 3
Ex Vivo Biodistribution Data of 2'-¹⁸F-Fluorofolic Acid at 75 Minutes After Injection in Nude Mice Bearing KB Tumor Xenografts

Organ or tissue	Control group (n = 3)	Antifolate group (n = 3)
Lung	0.55 ± 0.07	0.39 ± 0.09
Liver	8.64 ± 1.21	3.63 ± 0.52
Kidney	35.73 ± 0.25	14.05 ± 1.02
Brain	0.41 ± 0.03	0.28 ± 0.04
Heart	0.58 ± 0.07	0.41 ± 0.04
Spleen	1.57 ± 0.38	0.98 ± 0.08
Intestines	4.36 ± 1.52	3.31 ± 3.14
Bone	1.52 ± 0.15	0.94 ± 0.13
Blood	0.36 ± 0.06	0.20 ± 0.04
Urine	258.99 ± 78.45	111.39 ± 37.78
Feces	28.58 ± 36.99	14.28 ± 11.12
Gallbladder	72.11 ± 16.98	69.85 ± 22.40
KB tumor	11.50 ± 0.28	8.65 ± 3.05

In antifolate group, each animal received 400 μ g of pemetrexed 1 h before radiotracer. Data are expressed as %ID/g.

positive kidneys. The KB tumors and the kidneys were clearly visualized under control conditions, whereas uptake of 2'-¹⁸F-fluorofolic acid in both folate receptor–expressing tissues was inhibited under blockade conditions (Fig. 3). In line with the ex vivo biodistribution data, maximum-intensity projections of the PET data confirmed the favorable elimination pattern showing highest radioactivity concentrations in the urinary bladder, gallbladder, and intestines, whereas liver uptake was only moderate.

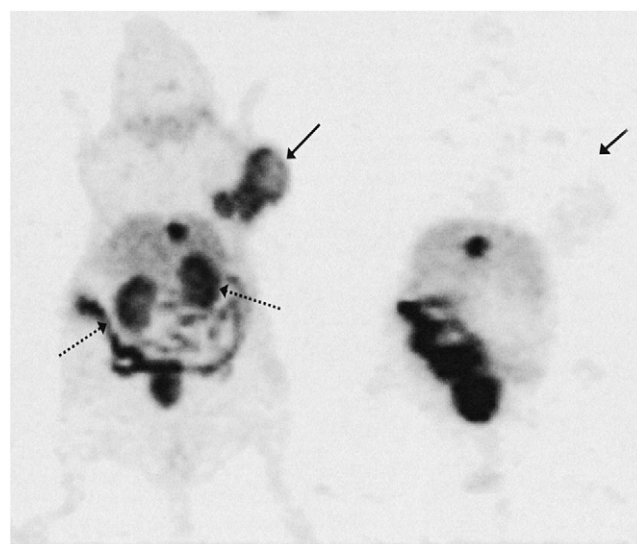


FIGURE 3. Maximum-intensity projection of PET data generated by injecting KB tumor-bearing mice (left: control; right: blockade) with 2'-¹⁸F-fluorofolic acid. Scan time: 75–105 min after injection. Arrows indicate KB tumors (bold arrows) and kidneys (dotted arrows).

TABLE 2

Results of Radiometabolite Analysis Using 2'-¹⁸F-Fluorofolic Acid in Nude Mice Bearing KB Tumor Xenografts

Sample	Metabolite (%) ($k' = 0.13$; $R_f = 0.37$)	Parent (%) ($k' = 1.06$; $R_f = 0.74$)
15 min		
Urine	82.1 ± 3.7	17.9 ± 3.7
Plasma	66.6 ± 4.3	33.4 ± 4.3
Tumor	61.1 ± 5.7	33.8 ± 5.2
90 min		
Urine	83.7 ± 6.3	12.8 ± 9.6
Plasma	63.0 ± 4.7	37.0 ± 4.7
Tumor	82.2 ± 13.2	17.9 ± 13.2

Animals were sacrificed 15 and 90 min after injection.

The excellent resolution of the dedicated small-animal PET system allowed visualization of a heterogeneous radioactivity distribution within the KB tumor xenografts (Fig. 4).

DISCUSSION

In the present study, we sought to apply an integrated approach whereby the bioisosteric replacement of hydrogen by a fluorine atom appeared attractive. Except for the high electronegativity, fluorine has a relatively small steric footprint that induces minimal steric perturbations. Thus, in contrast to previously developed folic acid conjugates, the novel candidate featured only minimal structural differences from folic acid.

Radiochemistry

Nucleophilic aromatic ^{18}F labeling via the fluoro-for-nitro exchange normally results in moderate to good radiochemical yields depending on the type of molecule (26). The precursor *N*²-(*N,N*-dimethylaminomethylene)-2'-nitro-folic acid di-*tert*-butylester used for the ^{18}F labeling in this study can be seen as a moderately activated aromatic system for nucleophilic substitution. The amide functionality in the *ortho*-position to the nitro leaving group acts as a moderate activating group (σ_p (–CONHMe) = 0.36 (27)), whereas the amine moiety in the *meta*-position is electron-donating and increases the electron density (σ_m (–NHMe) = –0.21 (27)). As a result, the modest activation enabled the fluoro-for-nitro exchange but required harsh conditions of high temperatures and prolonged reaction times, which in turn led to an extensive decomposition of the folic acid backbone as proven by HPLC analysis. Nonetheless, under optimized conditions of a 20-min reaction time at 140°C–145°C in dimethylformamide, the ^{18}F -labeled protected inter-

mediate was obtained in a maximum radiochemical yield of 8%. Several examples of (nonactivated) complex molecules labeled via nucleophilic aromatic substitution have been reported in radiochemical yields ranging from 1% to 5% (28,29). Considering the structural features and the molecular size of folic acid, the initial labeling yield of 8% (decay-corrected) and the isolated overall yield of approximately 4% (decay-corrected) reported in this study are acceptable.

Cleavage of the protecting groups was accomplished with 4 M HCl at 60°C in a reaction time of 12 min to afford 2'- ^{18}F -fluorofolic acid in 50% radiochemical yield. After purification by reversed-phase HPLC, the final product was formulated in physiologic phosphate buffer for biologic applications. The specific activity of the radiotracer was found to be 23.7 ± 12.2 GBq/ μmol , and the radiochemical purity was greater than 95%.

In Vitro and In Vivo Characterization

In vitro displacement experiments using KB tumor cells and ^3H -folic acid as radioligand revealed a K_i value of 1.8 nM, the highest in vitro binding affinity obtained so far in our group for fluorinated folates (19,20). In vivo PET studies in nude mice found highly specific uptake of 2'- ^{18}F -fluorofolic acid in the tumor as well as in the folate receptor–positive kidneys as demonstrated by blockade experiments (Fig. 3). The specificity of tracer uptake in the tumor and kidneys was also confirmed by ex vivo tissue counting and amounted to 87% and 81%, respectively. The brain, heart, and spleen also showed a notable blocking effect (Table 1). Besides the kidneys, a significant folate receptor expression has been reported for these tissues in BALB/c mice (30).

In ex vivo metabolite studies, only 1 hydrophilic radio-metabolite was observed besides the parent compound. Interestingly, the ratio of 2'- ^{18}F -fluorofolic acid and the metabolite in the plasma and urine did not significantly change between 15 and 90 min. In tumor tissue, the ratio of 2'- ^{18}F -fluorofolic acid to its radiometabolite decreased from 15 to 90 min because the percentage of radiometabolite was increasing over time.

In previous studies, the preadministration of the antifolate pemetrexed in combination with conjugated radio-folates labeled with metallic radionuclides ($^{99\text{m}}\text{Tc}$, ^{111}In , ^{177}Lu) reduced the kidney uptake by approximately 70%–80% (17,18). In this study, we also investigated the effect of preadministered pemetrexed for the first time in combination with an ^{18}F -labeled folate-based radiotracer. Ex vivo biodistribution data showed a clear reduction of kidney uptake by 61%. In contrast to the kidneys, tumor uptake of the radiotracer remained unaltered. Thus, the effect of pemetrexed on the kidney in this study was less pronounced but still remarkably high. Reduced radioactivity uptake in other excretion organs such as liver and intestines/feces was also observed in animals that received pemetrexed. Such a reduction in radioactivity accumulation in nontarget organs is highly desirable for PET.

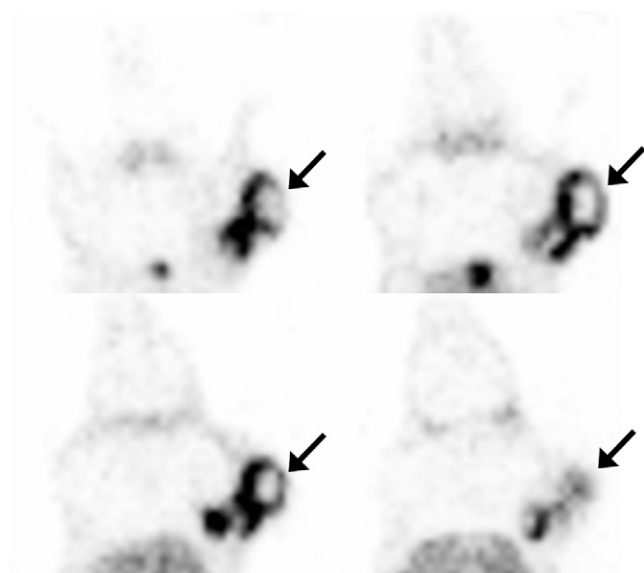


FIGURE 4. Representative series of horizontal PET images of control nude mouse bearing KB tumor xenograft. Images show head and thorax region including KB tumor in right shoulder (arrows). Animal was injected with 2'- ^{18}F -fluorofolic acid and scanned 75–105 min after injection.

The high resolution of the quad-HIDAC PET system and the excellent imaging characteristics of the new ^{18}F -labeled PET tracer allowed visualization of heterogeneous radio-tracer uptake in KB tumor xenografts.

Compared with our previously published ^{18}F -labeled folic acid derivatives, $2'$ - ^{18}F -fluorofolic acid provides superior imaging characteristics and outperforms previously reported ^{18}F -labeled folates (Supplemental Fig. 4). Whereas the absolute tumor uptake and the degree of specificity are in a similar range for all three ^{18}F -labeled folates, the new ^{18}F -labeled folate is characterized mainly by fast and efficient renal elimination and moderate hepatobiliary excretion.

Low intestinal tracer accumulation is crucial for the flawless detection of tumors and metastases near excretion organs. A tumor-to-bile ratio of 0.56 for $2'$ - ^{18}F -fluorofolic acid as determined in the ex vivo tissue sampling highlights the favorable elimination pattern of the new derivative, compared with α/γ - ^{18}F -FBA folate (0.025) and ^{18}F -click folate (0.0045). This favorability is also clearly visible from Supplemental Figure 4, where $2'$ - ^{18}F -fluorofolic acid shows the best target-to-background contrast.

CONCLUSION

$2'$ - ^{18}F -fluorofolic acid, a novel ^{18}F -labeled folic acid derivative created from an integrated ^{18}F -labeling approach, has been developed. The new radioligand exhibits high affinity and specificity for the folate receptor and outperforms previously developed ^{18}F -labeled radiofolates. To the best of our knowledge, $2'$ - ^{18}F -fluorofolic acid is so far the most promising ^{18}F -radioligand for imaging folate receptor-positive tumors.

ACKNOWLEDGMENTS

We thank Claudia Keller, Sabine Baumann, and Petra Wirth for their support and help with the in vivo and ex vivo experiments, and Andrea Weber and Phoebe Y.H. Lam for their work in the in vitro studies.

REFERENCES

1. Fox JT, Stover PJ. Folate-mediated one-carbon metabolism. In: Litwack G, ed. *Folic Acid and Folates*. Vol 79. Boston, MA: Academic Press/Elsevier; 2008:1–44.
2. Yuasa H, Inoue K, Hayashi Y. Molecular and functional characteristics of proton-coupled folate transporter. *J Pharm Sci*. 2009;98:1608–1616.
3. Jansen G. Receptor- and carrier-mediated transport systems for folates and antifolates. In: Jackman AL, ed. *Anticancer Drug Development Guide: Antifolate Drugs in Cancer Therapy*. Totowa, NJ: Humana Press Inc.; 1999:293–321.
4. Antony AC. Folate receptors. *Annu Rev Nutr*. 1996;16:501–521.
5. Elwood PC. Molecular cloning and characterization of the human folate-binding protein cDNA from placenta and malignant tissue culture (KB) cells. *J Biol Chem*. 1989;264:14893–14901.
6. Wu M, Gunning W, Ratnam M. Expression of folate receptor type α in relation to cell type, malignancy, and differentiation in ovary, uterus, and cervix. *Cancer Epidemiol Biomarkers Prev*. 1999;8:775–782.
7. Hilgenbrink AR, Low PS. Folate receptor-mediated drug targeting: from therapeutics to diagnostics. *J Pharm Sci*. 2005;94:2135–2146.
8. Leamon CP, Jackman AL. Exploitation of the folate receptor in the management of cancer and inflammatory disease. In: Litwack G, ed. *Folic Acid and Folates*. Vol 79. Boston, MA: Academic Press/Elsevier; 2008:203–233.
9. Ke CY, Mathias CJ, Green MA. Folate receptor-targeted radionuclide imaging agents. *Adv Drug Deliv Rev*. 2004;56:1143–1160.
10. Mathias CJ, Hubers D, Low PS, Green MA. Synthesis of [^{99m}Tc]DTPA-folate and its evaluation as a folate-receptor-targeted radiopharmaceutical. *Bioconjug Chem*. 2000;11:253–257.
11. Reddy JA, Xu LC, Parker N, Vetzal M, Leamon CP. Preclinical evaluation of ^{99m}Tc -EC20 for imaging folate receptor-positive tumors. *J Nucl Med*. 2004;45:857–866.
12. Müller C, Dumas C, Hoffmann U, Schubiger PA, Schibli R. Organometallic ^{99m}Tc -technetium(I)- and Re-rhenium(I)-folate derivatives for potential use in nuclear medicine. *J Organomet Chem*. 2004;689:4712–4721.
13. Siegel BA, Dehdashti F, Mutch DG, et al. Evaluation of ^{111}In -DTPA-folate as a receptor-targeted diagnostic agent for ovarian cancer: initial clinical results. *J Nucl Med*. 2003;44:700–707.
14. Mathias CJ, Wang S, Lee RJ, Waters DJ, Low PS, Green MA. Tumor-selective radiopharmaceutical targeting via receptor-mediated endocytosis of gallium-67-deferoxamine-folate. *J Nucl Med*. 1996;37:1003–1008.
15. Mathias CJ, Lewis MR, Reichert DE, et al. Preparation of ^{66}Ga - and ^{68}Ga -labeled Ga(III)-deferoxamine-folate as potential folate-receptor-targeted PET radiopharmaceuticals. *Nucl Med Biol*. 2003;30:725–731.
16. McMartin KE, Morshed KM, Hazen-Martin DJ, Sens DA. Folate transport and binding by cultured human proximal tubule cells. *Am J Physiol*. 1992;263:F841–F848.
17. Müller C, Schibli R, Krenning EP, de Jong M. Pemetrexed improves tumor selectivity of ^{111}In -DTPA-folate in mice with folate receptor-positive ovarian cancer. *J Nucl Med*. 2008;49:623–629.
18. Müller C, Schibli R, Forrer F, Krenning EP, de Jong M. Dose-dependent effects of (anti)folate preinjection on ^{99m}Tc -radiofolate uptake in tumors and kidneys. *Nucl Med Biol*. 2007;34:603–608.
19. Bettio A, Honer M, Müller C, et al. Synthesis and preclinical evaluation of a folic acid derivative labeled with ^{18}F for PET imaging of folate receptor-positive tumors. *J Nucl Med*. 2006;47:1153–1160.
20. Ross TL, Honer M, Lam PYH, et al. Fluorine-18 click radiosynthesis and preclinical evaluation of a new ^{18}F -labeled folic acid derivative. *Bioconjug Chem*. 2008;19:2462–2470.
21. Ametamey SM, Moser R, Ross TL, Groehn V, inventors. ^{18}F -labelled folates. European patent WO2008125617. October 23, 2008.
22. Missimer J, Madi Z, Honer M, Keller C, Schubiger PA, Ametamey SM. Performance evaluation of the 16-module quad-HIDAC small animal PET camera. *Phys Med Biol*. 2004;49:2069–2081.
23. Antony AC, Kane MA, Portillo RM, Elwood PC, Kolhouse JF. Studies of the role of a particulate folate-binding protein in the uptake of 5-methyltetrahydrofolate by cultured human KB cells. *J Biol Chem*. 1985;260:14911–14917.
24. Cheng Y, Prusoff WH. Relationship between the inhibition constant (K_i) and the concentration of inhibitor which caused 50 per cent inhibition (I_{50}) of an enzymatic reaction. *Biochem Pharmacol*. 1973;22:3099–3108.
25. Honer M, Brühlmeier M, Missimer J, Schubiger AP, Ametamey SM. Dynamic imaging of striatal D_2 receptors in mice using quad-HIDAC PET. *J Nucl Med*. 2004;45:464–470.
26. Coenen HH. Fluorine-18 labelling methods: features and possibilities of basic reactions. In: Schubiger PA, Lehmann L, Friebe M, eds. *PET Chemistry: The Driving Force in Molecular Imaging*. Berlin, Germany: Springer; 2007:15–50.
27. Hansch C, Leo A, Taft RW. A survey of Hammett substituent constants and resonance and field parameters. *Chem Rev*. 1991;91:165–195.
28. Lemaire C, Cantineau R, Guillaume M, Plenevaux A, Christiaens L. Fluorine-18-altanserin: a radioligand for the study of serotonin receptors with PET: radio-labeling and in vivo biologic behavior in rats. *J Nucl Med*. 1991;32:2266–2272.
29. Mathews WB, Murugesan N, Xia J, et al. Synthesis and in vivo evaluation of novel PET radioligands for imaging the endothelin-a receptor. *J Nucl Med*. 2008;49:1529–1536.
30. Parker N, Jo Turk M, Westrick E, Lewis JD, Low PS, Leamon CP. Folate receptor expression in carcinomas and normal tissues determined by a quantitative radioligand binding assay. *Anal Biochem*. 2005;338:284–293.



The Journal of
NUCLEAR MEDICINE

A New ^{18}F -Labeled Folic Acid Derivative with Improved Properties for the PET Imaging of Folate Receptor–Positive Tumors

Tobias L. Ross, Michael Honer, Cristina Müller, Viola Groehn, Roger Schibli and Simon M. Ametamey

J Nucl Med. 2010;51:1756-1762.

Published online: October 18, 2010.

Doi: 10.2967/jnumed.110.079756


This article and updated information are available at:
<http://jnm.snmjournals.org/content/51/11/1756>

Information about reproducing figures, tables, or other portions of this article can be found online at:
<http://jnm.snmjournals.org/site/misc/permission.xhtml>

Information about subscriptions to JNM can be found at:
<http://jnm.snmjournals.org/site/subscriptions/online.xhtml>

The Journal of Nuclear Medicine is published monthly.
SNMMI | Society of Nuclear Medicine and Molecular Imaging
1850 Samuel Morse Drive, Reston, VA 20190.
(Print ISSN: 0161-5505, Online ISSN: 2159-662X)

© Copyright 2010 SNMMI; all rights reserved.

 SOCIETY OF
NUCLEAR MEDICINE
AND MOLECULAR IMAGING